*Geologica Acta, Vol.11, Nº 3, September 2013, 359-370*
DOI: 10.1344/105.000001871
*Available online at www.geologica-acta.com*

geologica acta

# Physico-chemical analysis of Albian (Lower Cretaceous) amber from San Just (Spain): implications for palaeoenvironmental and palaeoecological studies

**J. DAL CORSO** [1] **G. ROGHI** [2] **E. RAGAZZI** [3] **I. ANGELINI** [1]

**A. GIARETTA** [2] **C. SORIANO** [4] **X. DELCLÒS** [5] **H.C. JENKYNS** [6]

[1] **Dipartimento di Geoscienze, Università degli Studi di Padova**
Via Gradenigo 6, 35131, Padova, Italy. Dal Corso E-mail: jacopo.dalcorso@unipd.it Angelini E-mail: ivana.angelini@unipd.it

[2] **Istituto di Geoscienze e Georisorse (IGG-CNR)**
via Gradenigo 6, 35131, Padova, Italy. Roghi E-mail: guido.roghi@igg.cnr.it

[3] **Dipartimento di Scienze del Farmaco, Università degli Studi di Padova**
L.go Meneghetti 2, 35131, Padova, Italy. E-mail: eugenio.ragazzi@unipd.it

[4] **European Synchrotron Radiation Facilities (ESRF)**
Rue Jules Horowitz, 6, 38000, Grenoble, France E-mail: carmen.soriano@gmail.com

[5] **Department d'Estratigrafia, Paleontologia i Geociències Marines, Facultat de Geologia, Universitat de Barcelona**
Martí i Franquès s/n, 08028 Barcelona, Spain. E-mail: xdelclos@ub.edu

[6] **Department of Earth Sciences, University of Oxford**
South Parks Road, Oxford OX1 3AN, UK. E-mail: hugh.jenkyns@earth.ox.ac.uk

## ABSTRACT

Amber from a Lower Cretaceous outcrop at San Just, located in the Eastern Iberian Peninsula (Escucha Formation, Maestrat Basin), was investigated to evaluate its physico-chemical properties. Thermogravimetric (TG) and Differential Thermogravimetric (DTG) analyses, infra-red spectroscopy, elemental and C-isotope analyses were performed. Physico-chemical differences between the internal light nuclei and the peripheral darker portions of San Just amber can be attributed to processes of diagenetic alteration that preferentially took place in the external amber border colonized by microorganisms (fungi or bacteria) when the resin was still liquid or slightly polymerized. $\delta^{13}C_{amber}$ values of different pieces of the same sample, from the nucleus to the external part, are remarkably homogeneous, as are $\delta^{13}C_{amber}$ values of the darker peripheral portions and lighter inner parts of the same samples. Hence, neither invasive microorganisms, nor diagenetic alteration, changed the bulk isotopic composition of the amber. $\delta^{13}C$ values of different amber samples range from -21.1‰ to -24‰, as expected for $C_3$ plant-derived material. C-isotope analysis, coupled to palaeobotanical, TG and DTG data and infra-red spectra, suggests that San Just amber was exuded by only one conifer species, belonging to either the Cheirolepidiaceae or Aracauriaceae, coniferous families probably living under stable palaeoenvironmental and palaeoecological conditions.

*KEYWORDS* | **Amber. C-isotopes. Thermogravimetric analyses. Infra-red spectroscopy. Cretaceous.**

## INTRODUCTION

Amber from an outcrop at San Just (Teruel Province) in the Iberian Peninsula (Fig. 1) represents a fossilized natural resin that originated in an Early Cretaceous forest (Peñalver and Delclòs, 2010). San Just amber is one of the richest known Early Cretaceous deposits for its biological inclusions, yielding fungal hyphae, trichomes of ferns or conifers, pollen grains, and many different arthropods such as arachnids and hexapods (Peñalver *et al.*, 2007; Peñalver and Delclòs, 2010). The horizons yielding amber derive from the Escucha Formation, that has been interpreted as deposited in shallow-marine to freshwater environments in the Maestrat Basin (Cervera *et al.*, 1976; Querol and Salas, 1988; Querol *et al.*, 1992; Peyrot *et al.*, 2007a,b; Delclòs *et al.*, 2007; Peñalver *et al.*, 2007). The Escucha Formation is composed of three members: a lower, a middle and an upper member (namely, Regachuelo, Barriada and La Orden Members). San Just Amber has been found in the organic-rich levels in the interval extending from the top of the Regachuelo Member to the base of the La Orden Member, corresponding to freshwater swamp facies (Querol *et al.*, 1992; Peñalver *et al.*, 2007; Villanueva-Amadoz *et al.*, 2010) and recently dated to the middle–early late Albian based upon angiosperm pollen (Villanueva-Amadoz *et al.*, 2010). The amber is associated with abundant conifer remains belonging to the Cheirolepidiacean conifer *Frenelopsis* (Peñalver *et al.*, 2007; Alcalá *et al.*, 2009). Although many previous studies have suggested that the association *Frenelopsis*–amber characterises brackish and estuarine environments (Gomez *et al.*, 2008; Néraudeau *et al.*, 2003, 2005, 2009; Peyrot *et al.*, 2005a), in the Cretaceous of Spain *Frenelopsis* is also found in freshwater environments (Gomez *et al.*, 2001; Gomez *et al.*, 2002; Villalba-Breva *et al.*, 2012). San Just amber is also associated with fossils plant macro-remains and sporomorphs of ferns, Ginkgoales, Bennettitales, Caytoniales, Cycadales, Coniferales and angiosperms, which together suggest warm and humid environmental conditions (Gomez *et al.*, 1999, 2000; Gomez 2002; Díez *et al.*, 2005; Sender *et al.*, 2005; Peyrot *et al.*, 2005b, 2007a,b; Villanueva-Amadoz *et al.*, 2010). An Araucariacean palaeobotanical affinity has been suggested for San Just amber by Peñalver *et al.* (2007) by comparison with other Spanish amber localities (Alonso *et al.*, 2000; Chaler and Grimalt, 2005). However, the presence of abundant Cheirolepidiacean plant remains in the San Just deposits and comparison with other Lower Cretaceous amber-bearing outcrops from western Spain (Menor-Salvan *et al.*, 2010; Najarro *et al.*, 2010) could also suggest a Cheirolepidiacean paleobotanical affinity. Existing data show that San Just amber can clearly be attributed to conifers, but the attribution to a specific conifer family, most likely Cheirolepidiaceae or Araucariaceae, is not possible yet.

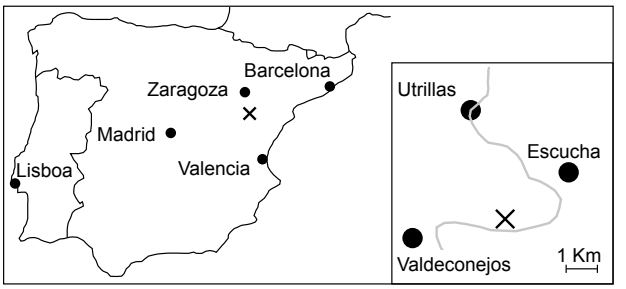


**FIGURE 1** | Map of the study area. Right panel: location of the study area. San Just amber deposit is represented by an X.

San Just amber typically shows a peripheral portion darker than the nucleus and opaque (Peñalver *et al.*, 2007). Peñalver *et al.* (2007) observed filamentous structures by optical and scanning electron microscope. These structures are abundant in the more external part of the peripheral portion and scarcer towards the boundary with the inner and lighter part of the amber, and were first interpreted as alteration/degradation structures (Peñalver *et al.*, 2007). However, similar structures are present in the outer part of many other Cretaceous amber that have been described as colonies of fossil fungi (Ascaso *et al.*, 2005) or bacteria (Breton and Tostain, 2005; Schmidt and Schäfer, 2005; Breton, 2007). Nevertheless, diagenetic alteration and the effects of microbiological intervention can coexist.

To investigate this issue further we decided to further explore some physico-chemical properties (thermal behaviour, infra-red spectra, elemental composition and C-isotope signature) of San Just amber, in order to understand the changes from the darker peripheral portion of the amber, and whether degradation or microbiological inclusions produced the peripheral zones. In addition, the C-isotope signature of San Just amber was also studied to determine the ecology and the environmental conditions of the resin-producing plants. It has been pointed out that the $\delta^{13}C$ signature of amber could be a useful tool for palaeobotanical, palaeoclimatic and palaeoenvironmental purposes (Nissenbaum and Yakir, 1995; Murray *et al.*, 1998; Nissenbaum *et al.*, 2005; McKellar *et al.*, 2008, 2011; Dal Corso *et al.*, 2011). The C-isotope signature of amber is the result of a complex series of carbon-fractionation processes involving $CO_2$ taken up by plants from the atmosphere. During photosynthesis the following factors influence the C-isotope fractionation of $C_3$ plants (the only metabolic group assumed to be present during the Cretaceous): i) The carbon-isotope composition of the atmosphere ($\delta^{13}C_{atm}$); ii) Diffusion of $CO_2$ from the air into the leaves (-4.4‰); iii) Biochemical fractionation during carboxylation (-27 to -29‰); and iv) Ecological factors, such as water stress (+3 to +6‰), nutrient shortage (-4‰),

light limitation (-5 to -6‰) and low temperature (-3‰) (Arens *et al.*, 2000; Dal Corso *et al.*, 2011 and references therein). Carbon isotopes are further fractionated during the biosynthesis of specific plant compounds: with regard to amber, diterpenoids of probable resin origin have higher values compared with associated coals (+1 to +2‰) and with triterpenoids derived from plant epicuticular waxes (+2 to +4‰) (Schoell *et al.*, 1994). Moreover, insect infestation has been recently linked to an observed 1‰ enrichment of modern and fossil resin $\delta^{13}C$ in a similar way to the $^{13}C$ enrichment in resin of plants living under water-stress conditions (McKellar *et al.*, 2011). Thus, the C-isotope signatures of $C_3$ plants vary widely (from approximately -20‰ to -35‰; *e.g.* Cerling and Harris, 1999), depending on a combination of physical, biochemical and ecological factors. Large $\delta^{13}C$ variability has been also observed in amber (*e.g.*, McKellar *et al.*, 2008; Dal Corso *et al.*, 2011). Although the high $\delta^{13}C$ variability of amber could make the building of reliable $\delta^{13}C_{amber}$ curves for chemostratigraphic studies difficult, this geochemical variability itself can offer information about the ecology of resin-producing plants and the environmental conditions under which they grew.

## MATERIALS AND METHODS

Amber analysed in this study derives from an outcrop named San Just (acronym SJU), located near Escucha village (Fig. 1) (Peñalver and Delclòs, 2010). Absolute ages are given according to the International Stratigraphic Chart (International Commission on Stratigraphy 2012, available at: http://www.stratigraphy.org/) and Gradstein *et al.* (2012).

### Thermogravimetric (TG) and differential thermogravimetric (DTG) analyses

TG and DTG profiles were obtained for each sample using a prototypal C.N.R. instrument (I.G.G. C.N.R., Padova, Italy) named "Le Chatelier". A type S (Pt-10% Rh/Pt) thermocouple placed inside an electric furnace provided sample and furnace measurements. Amber pieces were taken from both the darker peripheral portion and the lighter internal part of fossil resins. These pieces were pulverized in an agate mortar before measurement (mass 500mg, particle size <75$\mu$m) and inserted into a platinum crucible, placed on a quartz glass support interfaced with a Mettler Toledo AB 104 balance. The heating rate was 10°C/min in air, starting from room temperature (20°C) and reaching a maximum temperature of 700°C. The ash residue was 3.45±1.66 wt% (mean±1SD), and the range was 0.74% to 5.4%. A computer, equipped with custom-made software written in Lab View 5.1 language recorded sequential temperature and weight for each sample (TG signal) and derived DTG data from the recorded TG signal. The Main Thermal Point (MATHEP) from the DTG data corresponding to the maximal rate of weight loss was used as a comparison parameter, as previously described (Ragazzi *et al.*, 2003, 2009).

### Elemental analysis

A CE-Instruments EA 1110 Automatic Elemental Analyser, equipped with AS 200 autosampler and Mettler Toledo AT21 Comparator, was used. The instrument consists of a simultaneous carbon–hydrogen–nitrogen and sulphur analyser based on reliable dynamic flash combustion and GC separation (with helium as carrier gas), followed by thermal conductivity detectors (TCD). A workstation, which permits complete automation from weight entry to storage of results, consists of Eager 200 Software installed on a compatible XT/AT microcomputer with a graphic printer. The Eager 200 Software offers the possibility of using K factors and linear regression for calculation. Weight entry via the RS 232CC link is fully automated. The powdered sample (about 2mg) was placed into a tin capsule and loaded into the AS 200 autosampler. The calibration standards for carbon–hydrogen–nitrogen and sulphur were prepared from known amounts of sulfanilamide ($C_6H_8N_2O_2S$).

### Infra-red spectroscopic analyses

Small amber pieces were cut from selected amber samples after a careful optical microscopy study. The aim of this preliminary work was to obtain pieces from each amber sample representative of the areas showing different physical characteristics (*i.e.* colour, opacity and presence of inclusions). The pieces were analysed with Diffuse-Reflectance Infra-Red Fourier Transform (DRIFT) using a Nicolet NEXUS 760 FTIR instrument, equipped with a Collector II accessory. Infra-red spectra were recorded in the spectral range 4000–400cm$^{-1}$, with a resolution of 4cm$^{-1}$, using 64 scans accumulation. The data were processed with the Nicolet Instrument Corporation program: OMNIC, version 5.1. The DRIFT analysis was performed on very small amounts of amber (0.2mg), using a micro-cup. The amber pieces were mixed with 20mg of dry KBr, ground in an agate mortar, and the mixture was placed directly into the sample holder.

### Carbon-isotope analyses

Separated pieces of San Just amber samples were crushed into a fine powder and treated with 3M HCl in order to remove possible microscopic residual carbonates deriving from the amber-bearing sediment. A fixed mass of this powder (1.5mg) was placed in a tin capsule. $\delta^{13}C$ analyses were performed at the Research Laboratory

for Archaeology and the History of Art (University of Oxford) with a Carlo Erba NA 1108 elemental analyser coupled to a SERCON Geo 20/20 IRMS running in continuous flow mode with a He carrier gas (flow rate 100ml/min). The instrumental precision was determined as the standard deviation of an alanine in-house standard ($\delta^{13}C_{alanine}$=-26.94±0.14‰, n=43) routinely checked against international standards IAEA-CH-6 and IAEA-CH-7 and traceable back to the VPDB standard.

## Statistical analysis

Data are expressed as mean ±SD. For correlation analysis of thermal data, we measured the Pearson correlation coefficient R in order to find a measure of dependence between the geological age and the value of the Main Thermal Point (MATHEP). It is well known that the Pearson correlation coefficient R indicates the strength of a linear relationship between two variables; it should be taken into account that the value of R cannot completely characterize the relationship between the two considered variables.

The thermal behaviour of the fossil resin may depend on different factors such as the age of the sample, degree of polymerization, chemical composition, diagenetic alteration and palaeobotanical origin. Thus, it is not possible to obtain a unique model for estimating the age of the sample on the basis of the DTG peak data. As already underlined in previous investigations (Ragazzi *et al.*, 2003, 2009), the thermal method should be seen as a complementary technique to be used together with other methods of age determination. It is best used as an overall method for the estimation of resin maturation, including any process that might be involved in taphonomic modification.

We did not use the coefficient of determination $R^2$, which represents the proportion of variance explained by the model ($R^2$ can also be taken as a measure of how good a predictor might be if constructed from the modelled values. Since several variables are involved, including physico-chemical and taphonomical ones, it is not possible to expect a direct prediction of the age just by means of this model).

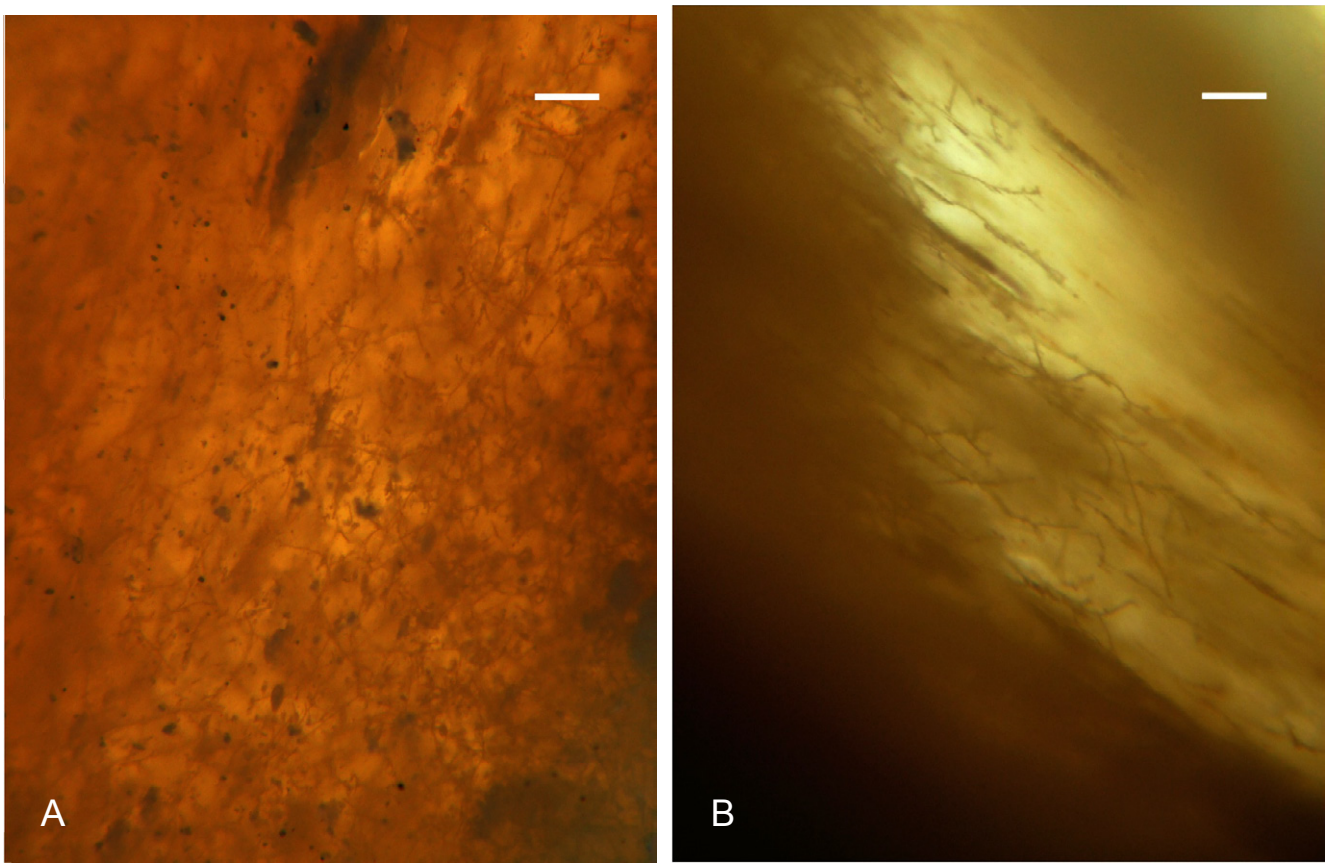


**FIGURE 2** | Filamentous structures in San Just amber (SJU 8 sample). A) Peripheral darker portion, B) border between the peripheral darker portion and the inner lighter portion. White bar = 50µm.

## RESULTS AND DISCUSSION

Pieces of San Just amber samples were initially checked under the optical microscope to observe the differences between the darker peripheral and the lighter inner portions. Filamentous structures are very abundant in the darker peripheral part and become less abundant approaching the border with the inner lighter nucleus (Fig. 2A, B), as already described by Peñalver *et al.* (2007). These structures are very similar to the filaments described by other authors as microbiological inclusions (Ascaso *et al.*, 2005; Breton and Tostain, 2005; Schmidt and Schäfer, 2005; Breton 2007), and in particular to the fungal hyphae found in the Lower Cretaceous Álava amber by Ascaso and colleagues (Ascaso *et al.*, 2003, 2005). As observed by Schmidt and Dilcher (2007 and references therein) in modern examples these fungal hyphae or bacteria can grow in liquid resin. However, it has been postulated that filamentous microorganisms can also grow on the surface when resin is already solidified, producing a thin dark peripheral crust (Néraudeau *et al.*, 2011). The fact that we observe a pervasive colonization in San Just amber (Fig. 2B) suggests that fungi or bacteria invaded the soft resin while it was sitting in water or on wet soil.

### Thermogravimetric (TG) and differential thermogravimetric analyses (DTG)

Data obtained from thermal analyses of the samples of Albian amber found in the San Just area are shown in Table I (Electronic Appendix available at www.geologica-acta.com), Figure 3 and Figure 4. The TG and DTG curves show unambiguous patterns with an overall three-phase profile (Figs. 3, 4). Two samples were investigated; one (SJU6) presented a minimal alteration surface, whereas the other (SJU8) showed the common two-coloured appearance, with a darker outer part and a lighter nucleus. The MATHEP values of the analysed pieces obtained from the sample SJU6 ranged from 412 to 422°C (see Table I), and represented the loss of more than 70% of the sample. The remaining mass of the sample was lost above 450°C, showing some minor peaks (secondary peaks) between 351 and 616°C.

The external characteristics of sample SJU8 are shown in Figure 4A. TG profiles of the peripheral portion (P) and inner part (I) of San Just amber (sample SJU8) are presented in Figure 4B. The TG profile of the inner amber portion is similar to the profile of sample SJU6 presented in Figure 3, showing the same pattern with three main DTG peaks (Fig. 4, SJU8.2G and SJU8.4G). On the other hand, the TG profile of the darker peripheral portion (Fig. 4, SJU8.1A and SJU8.3A) presents an almost single-phase pattern, from 250 to 650°C, and a DTG profile characterized by the presence of several peaks, which are difficult to assign

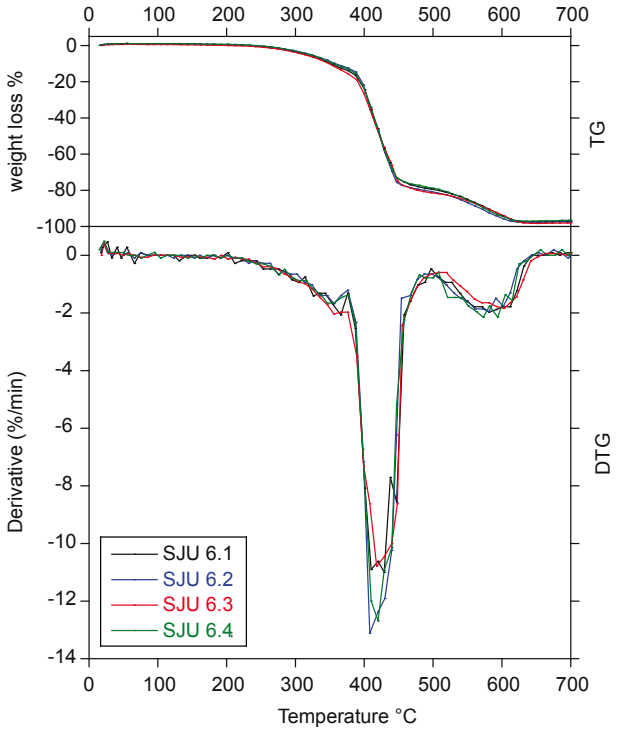


**FIGURE 3** | Thermogravimetric (TG) and Differential Thermogravimetric (DTG) profiles of specimens from SJU 6 amber samples. Characteristics of the specimens are shown in Table I.

to any major component, although an apparent maximum is detectable in the range 314–352°C and 551–575°C (see secondary peaks in Table I).

### Elemental analysis

The elemental composition of San Just amber samples is presented in Table II. The carbon content is around 78–79 wt%, hydrogen content ranges around 11–12 wt%, oxygen and trace elements are about 9%, sulphur between 0.45–0.65 wt%, and nitrogen is present in traces (0.03 wt%).

### Infra-red spectroscopic analysis

Eleven amber samples from San Just were analysed by DRIFT. Amber pieces from the inner and the peripheral portions of studied samples were analysed. The DRIFT spectra of the inner light amber portions show similar features for all samples (see the typical spectra in Fig. 5, black line). The main peaks are due to the C–H bonds, as expected for a fossil resin (Langehneim and Beck, 1965). In particular, the more intense bands are at: i) 2929±3cm$^{-1}$ and 2947±3cm$^{-1}$ (shoulder), due to the asymmetric stretching of the $CH_2$ and $CH_3$ bonds; ii) 2868±1cm$^{-1}$ and 2852±2cm$^{-1}$ (shoulder), due to the symmetric stretching of the $CH_2$ and $CH_3$ bonds; and iii) 1456±1cm$^{-1}$ and 1376±1cm$^{-1}$, due to the bending of the $CH_3$ and $CH_2$ bonds.

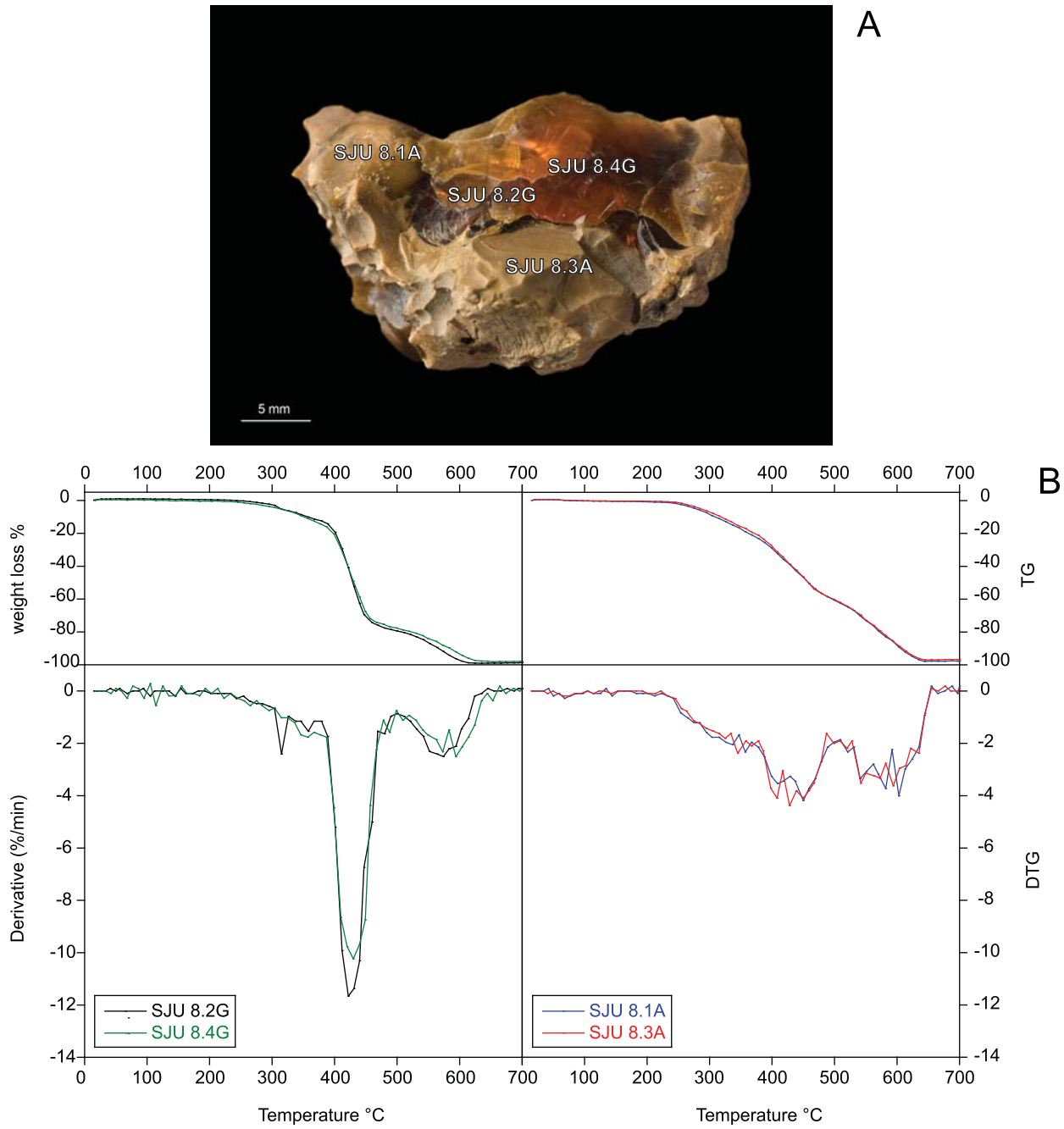


**FIGURE 4** | A) SJU 8 amber specimens: position of sub-samples analysed for $\delta^{13}C$ and thermogravimetry. B) comparison between TG and DTG profiles of the lighter inner portions (left graph) and the darker peripheral ones (right graph) of the four specimens.

A strong absorption band is present at about 1700cm$^{-1}$ and is assigned to carbonyl stretching. The intensity of this peak is higher or comparable to the intensity of the C–H bending peaks. Moreover, this peak is composed of several poorly resolved bands: it shows the main absorption at 1720±3cm$^{-1}$ and a shoulder (or rarely, a second separable peak) at 1701±3cm$^{-1}$. In a few cases, the absorption at 1701±3cm$^{-1}$ shows similar or slightly higher intensity than the peak at 1720±3cm$^{-1}$. A rather intense broad band is present in the DRIFT spectra at about 3450cm$^{-1}$ and is related to the OH stretching of alcohols and carboxylic acids. The possibility that the absorption at about 3450cm$^{-1}$ is influenced by the presence of water in the KBr may be ruled out because of the use of dried material, the record of a reference background before collection of each spectrum, and the relatively short time needed for a DRIFT analysis when compared with the classic preparation and analysis with KBr pellets.

In the range between 1300-900cm$^{-1}$, three intense peaks (with several shoulders) and two weak peaks have been systematically observed, respectively at 1227±1cm$^{-1}$, 1160±3cm$^{-1}$, 1032±1cm$^{-1}$ (intense), 1095±1cm$^{-1}$ and 975±1cm$^{-1}$ (weak). This spectral zone is difficult to interpret, since the absorption bands could be due to numerous different vibrations, namely: the C–O stretching of esters, alcohols and carboxylic acids, and the C–H out-of-plane vibrations of several structures. Comparing the DRIFT spectra obtained with previous work (Beck, 1970; Derrick *et al.*, 1999; Guiliano *et al.*, 2007) the bands at 1227±1cm$^{-1}$, 1160±3cm$^{-1}$, 1032±1cm$^{-1}$ could be tentatively assigned, respectively, to C–O stretching of carboxylic acids (Guiliano *et al.*, 2006); C–O stretching of aliphatic esters; and symmetric bending of the C–H cyclohexane (Beck, 1970) or C–O stretching (Guiliano *et al.*, 2006). A few very weak peaks are also present in the range of 850–700cm$^{-1}$. The dark peripheral portions show DRIFT spectra similar to those obtained from the inner lighter part (Fig. 5), the main differences being related to changes in the intensity of the bands at about 1700cm$^{-1}$ (in several samples the peak shows a unique absorption at 1713±4cm$^{-1}$); 1032±1cm$^{-1}$ (more intense in the dark peripheral portion) and 975±1cm$^{-1}$ (weaker in the dark peripheral portion). Only two samples illustrate changes in the range of 1250–1150cm$^{-1}$; they do not display strong peaks but only broad absorption.

The carbonyl absorption band in the DRIFT spectra of San Just amber is complex and not easy to resolve. Consequently, in order to enhance the resolution, deconvolution and second derivative processes have been applied to the spectra (Fig. 6A, B). After deconvolution, all but two of the spectra show only two main peaks: at 1724±3cm$^{-1}$ (1726±5cm$^{-1}$ using the second derivative) and at 1698±4cm$^{-1}$. These bands are due, respectively, to ketone and carboxylic acid groups. Only in two spectra is a shoulder of the ketone band discernible at about 1735–1745cm$^{-1}$; this absorption is due to the presence of esters.

The main characteristics of the San Just amber spectra are the high intensity of the peak at 1032±1cm$^{-1}$ and the good resolution of the peak at 975±1cm$^{-1}$ (generally only a shoulder in the FTIR spectra on numerous other amber varieties). Other characteristic but weak and unassigned peaks are present at 888±1cm$^{-1}$ (commonly only a small shoulder), 856±1cm$^{-1}$ and 814±1cm$^{-1}$. The band at about 888cm$^{-1}$ in the infra-red spectra of fossil resin is usually attributable to out-of-plane C–H bending in the exocyclic methylene groups. These groups also give bands at 3050–309cm$^{-1}$ and 1640cm$^{-1}$ (Beck, 1970; Derrick *et al.*, 1999; Guiliano *et al.*, 2007). Even though a very small absorption is present at 888cm$^{-1}$ in the spectra of San Just ambers, the other associated peaks are not apparent, so

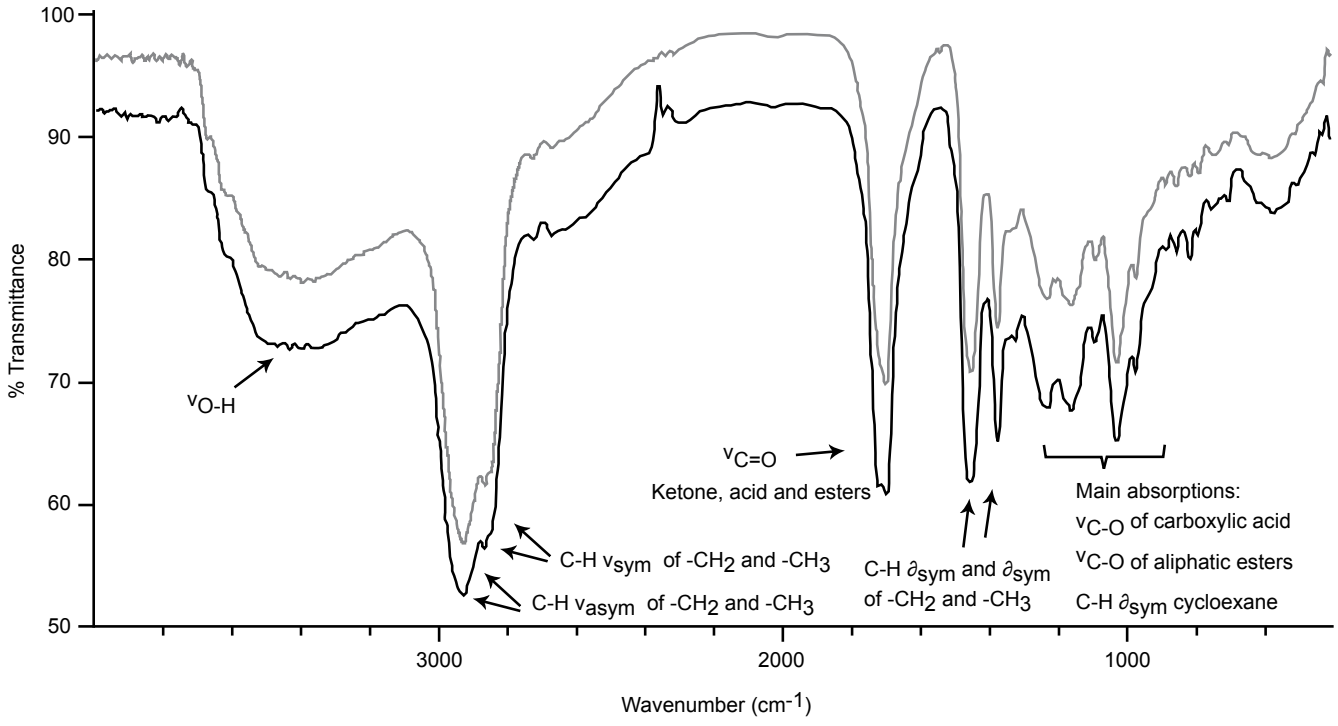


**FIGURE 5** | DRIFT spectra (transmittance mode) of two fossil resin specimens from the SJU8 amber sample: a specimen from the darker peripheral portion (grey line) and a specimen from the lighter inner part of the sample (black line). The assignments of the main absorption peaks are reported. (The black spectrum was translated along the y-axis in order to display both spectra properly).

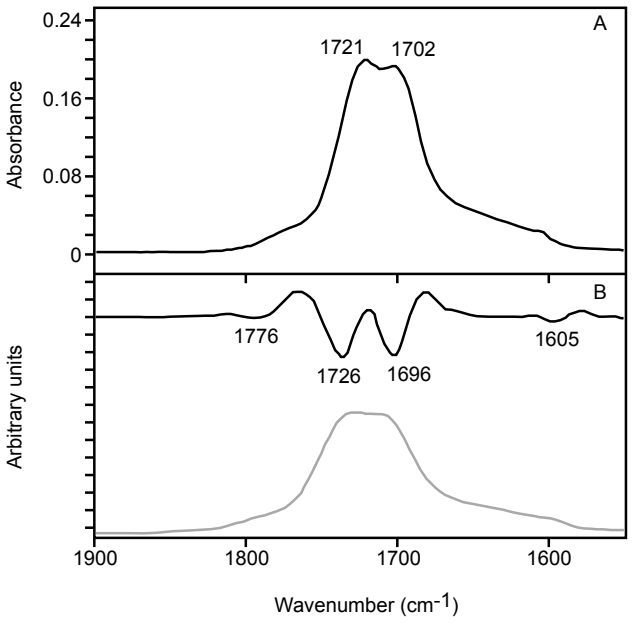


**FIGURE 6** | DRIFT spectra (absorbance mode) of sample SJU6 in the range of 1900–1550 $cm^{-1}$. A) DRIFT spectrum after deconvolution; B) DRIFT spectrum (grey line) and second derivative (black line).

we may exclude the presence of terminal olefin. Previous Raman studies have proved that the amount of exocyclic methylene groups decrease with increasing maturation of the fossil resin (Edwards and Farwell, 1996; Winkler *et al.*, 2001; Brody *et al.*, 2001). The amber from San Just, as suggested in a previous work (Peñalver *et al.*, 2007), has a high degree of maturation.

## Carbon-isotope composition

Several pieces obtained from seven amber samples from the San Just outcrop were analysed for the $\delta^{13}C$. These amber pieces show $\delta^{13}C$ values ranging from -21.1‰ to -24‰ (Table III), with a mean ±1SD of -22.5±1.01‰, falling within the range expected for $C_3$ plant-derived material. C-isotope values of different amber pieces within the same sample are very similar, as shown for SJU5, SJU6 and SJU8 samples (Table III). Moreover, analyses performed on the darker peripheral portion and on the inner lighter portion of single samples (SJU6 and SJU8) did not show any significant differences in the C-isotope signature.

## Physico-chemical differences between peripheral portions and nuclei of San Just amber

Lighter inner portions of amber from San Just show similar TG profiles and MATHEP values, ranging from 412 to 429°C. Previous studies have shown that the MATHEP values of amber are correlated with their age and maturation (Ragazzi *et al.*, 2003, 2009). San Just amber presents MATHEP values that agree with the previously reported age *vs* MATHEP correlation (Ragazzi *et al.*, 2003, 2009) and confirm that MATHEP values seem to increase with increasing age (R=0.68, Fig. 7): this pattern may be due to the palaeobotanical origin of the resin, but it has also been explained by differences in chemical groups and bonds occurring with age, probably depending on the maturation process of resin (Ragazzi *et al.*, 2003). According to this model, MATHEP values observed for San Just amber would represent a higher degree of maturation than younger ambers (Fig. 7), in agreement with the results of infra-red spectral analysis (see infra-red spectroscopic analysis paragraph). By contrast, TG analyses of the darker peripheral amber portions yield results that are more difficult to interpret. The TG profile of the peripheral portion of San Just amber sample (SJU 8) shows an almost linear weight loss between 300 to 600°C, that led to a less-defined DTG profile than those of the nuclei (Fig. 4). SJU 6 amber sample probably experienced a minor degree of alteration, since TG and DTG profiles of the darker peripheral portion are very similar to the TG and DTG profiles of the inner lighter part (Fig. 3).

Infra-red analyses of external weathered crusts and internal parts of Upper Albian and Lower Cenomanian French amber samples were carried out by Néraudeau *et al.* (2011). Although relative spectra and absorption peaks are not directly discussed, the authors did not find any significant variation in the FTIR spectra. Infra-red spectral analyses of the peripheral and internal portions of San Just amber samples (this study and Peñalver *et al.*, 2007) suggest that there are few differences in terms of

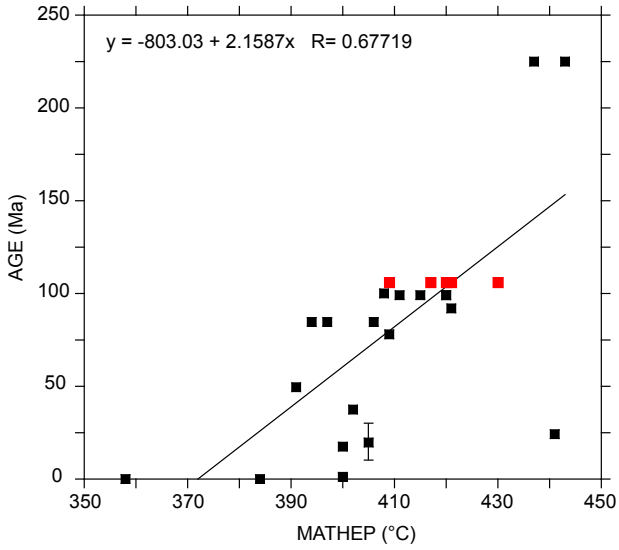


**FIGURE 7** | MATHEP *vs* AGE plot. Red squares: San Just amber, black squares: data from Ragazzi *et al.* (2003 and 2009) obtained from various samples of amber from different geological contexts.

the compounds present. DRIFT spectra of the peripheral and inner samples are very similar, suggesting a small degree of chemical transformation, differing mainly in the intensity of bands due to C–O and C=O bonds. This result is consistent with oxidation and degradation processes that may act in the outer part of the amber. As a result of these processes, the amounts and the types of functional groups containing double bonds and O may change. Thus, the present observation of shoulder loss and flat TG profile in the darker peripheral portion of the amber (Fig. 4) can be here interpreted as the effect of oxidation and/or diagenetic transformation, with possible rearrangement of chemical bonds originally present among the main components.

As previously stated, the difference in colour between the darker peripheral part and the inner lighter part of many San Just amber samples, and the presence of filamentous structures, have been interpreted as evidence for some kind of alteration/degradation of the original fossil resin or related to the presence of poorly defined biological inclusions (Peñalver *et al.*, 2007). Our observations support the presence of microbiological inclusions, most likely fungal hyphae (Fig. 2). However, our physico-chemical data equally indicate that alteration has occurred. Of course, the two hypotheses are not mutually exclusive. The most likely model to explain the alteration in the peripheral part is: i) soft resin was originally colonized by microorganisms (fungi or bacteria) growing into the resin mass; ii) upon solidification of the resin, the microorganisms stopped growing; and iii) amber was subsequently buried by sediment, whereupon the portion containing the microorganisms was preferentially altered because the biological structures present facilitated diagenetic processes such as oxidation (due to several factors such as UV rays, salt, etc.). Indeed, fine tubules made by the activity of microorganisms would have increased the resin area exposed to weathering agents and would have speeded up oxidation. Supporting this assertion is the fact that the altered peripheral zones of the amber correspond exactly to the portion containing the microbiological filamentous structures.

The C-isotope composition of separated peripheral and inner pieces belonging to the same amber sample is very similar (Table III). It appears that the transformation of the main components in San Just amber, as suggested by TG profiles and DRIFT analyses, did not affect its C-isotope composition (Table III). Hence, during the alteration processes, the system must have remained closed with respect to carbon isotopes. Moreover, the microbiological inclusions did not change the bulk C-isotope composition of the amber. Fungal hyphae and bacteria incorporated in modern resin use the compounds present as a substrate to grow (Schmidt and Dilcher, 2007 and references therein). Consequently, the biological processes acting within a closed system prevent any significant C-isotope fractionation. If externally grown fungi had been incorporated in the fluid resin, a difference in C-isotope composition of amber in the fungus-containing areas might have been observed.

It is also interesting to note that the sulphur content in San Just amber is approximately 0.5wt% (Table II). This value is much lower than the sulfur content found in coals coming from the Alliaga-Utrillas sub-basin (6.15wt%: Querol *et al.*, 1992), actually the same depocentre that yielded the San Just amber. It seems likely that the amber was not affected by any post-depositional invasion of sulphur, unlike other organic substrates such as wood. This observation supports the hypothesis that the amber structure remained closed during its geological history and little or no transfer of elements from the surrounding sediment has occurred.

## Physico-chemical variability of San Just amber

It is known that fossil resin from the same deposit can be compositionally different: *e.g.* Lower Cretaceous ambers from Álava show different infra-red spectra and high variability in chemical composition (Alonso *et al.*, 2000; Chaler and Grimalt, 2005). However, all analysed San Just amber specimens exhibit similar and peculiar physico-chemical features. TG and DTG profiles of SJU-6 and SJU-8 samples, excluding data from the altered portions, have a very similar shape and MATHEP (Fig. 3; Fig. 4). These two samples also show similar infra-red spectra: both the absorption frequencies and the relative intensity of the bands are comparable in all the samples.

San Just amber $\delta^{13}C$ values vary over a range of 2.9‰ (from -21.1‰ to -24.0‰). When compared with recent gymnosperm resin, this variability is similar to that obtained by Stern *et al.* (2008) for a comparable number of resin samples produced by *Pinus sylvestris* trees growing in the same English localities and sampled at the same altitudes. The range of modern resin $\delta^{13}C$ values becomes larger if all the sampled localities are considered together, and/or if different *Pinus* species are examined (Stern *et al.*, 2008). Such a pattern could be reasonably linked to the effect that local environmental conditions have on plant carbon-isotope signatures.

A number of ecological factors can influence $^{13}C/^{12}C$ fractionation during $C_3$ photosynthesis. If these factors (*e.g.* water availability, temperature, salinity) are different (or change through time), the $\delta^{13}C$ of plants that assimilate atmospheric $CO_2$ with the same C-isotope composition will be different. Since amber has a strong potential to retain its pristine C-isotope signature, it is possible to

make comparisons with the behaviour of modern resin C-isotope values (this study, Dal Corso *et al.*, 2011, McKellar *et al.*, 2011). McKellar *et al.* (2008) tried to explain the highly variable $\delta^{13}C$ of Cretaceous Canadian amber. They reported a range of 4.8‰ for 13 amber samples from the Campanian Cedar Lake deposit, and 6.2‰ for 28 amber samples from the coeval Campanian Grassy Lake deposit, and linked such a wide variability to variable forest conditions and stressed plants. The comparison of San Just amber C-isotope variability with modern resin C-isotope ranges suggests that San Just amber was exuded by plants, possibly a conifer species (see introduction for a discussion on San Just amber botanical affinity), growing under stable environmental conditions. As previously noted, San Just amber is concentrated in a sedimentary facies of the Escucha Fm. that has been interpreted as formed in a freshwater swampy plain where the conifer forest probably grew under stable ecological/climatic conditions and the resin experienced limited or no transport.

## CONCLUSIONS

The integrated data presented here add useful information to our understanding of fossil resin of the San Just deposit.

i) TG, DTG analyses and infra-red spectra show that differences between the darker periphery and inner part of San Just amber are due to diagenetic alteration/degradation concentrated in those zones where microbiological inclusions are present. Diagenetic alteration took place primarily in the external parts of the amber lumps that had been colonized by microorganisms when the resin was still liquid. The presence of microbiological inclusions probably made the peripheral amber portion more susceptible to diagenetic alteration.

ii) Amber could retain its pristine C-isotope composition, even if it had experienced some diagenetic alteration during burial in sediments. Moreover, fungal hyphae or bacteria, observed in the peripheral darker portion of some San Just amber samples, did not change the bulk $\delta^{13}C_{amber}$ signature, supporting the hypothesis that they used enclosing compounds to grow into the soft resin. Thus, amber can be suggested as a tool for palaeoenvironmental, palaeoecological and palaeoeclimatic reconstructions based on its $\delta^{13}C$ signature, as it seems to represent a closed system with respect to C-isotopes as soon as it polymerizes.

iii) MATHEP data obtained from the light inner nuclei of San Just amber fit with the MATHEP *vs* age correlation of Ragazzi *et al.*, 2008, 2009.

iv) All TG and DTG profiles and infra-red spectra of samples SJU-6 and SJU-8 have similar characteristics, suggesting that San Just amber is chemically and physically homogeneous within the deposit. Moreover, a comparison with $\delta^{13}C$ variability data of modern gymnosperm resin, coupled with palaeobotanical information, suggests that the San Just amber was produced by a single conifer species living under stable environmental conditions.

## ACKNOWLEDGMENTS

The authors would like to thank Peter Ditchfield for isotope analyses at the Research Laboratory for Archaeology and the History of Art (University, of Oxford, UK), Alessandro Pavese (University of Milan, Italy) for supporting the use of the IR instrument and Sandra Boesso (Università degli Studi di Padova, Italy) for TG analyses. Thanks go to Nereo Preto (Università degli Studi di Padova, Italy) for useful suggestions and a pre-revision of the manuscript. We thank Didier Néraudeau and an anonymous reviewer for their comments that greatly improved the manuscript. This study has been partially funded by the CGL2011–23948/BTE "The Cretaceous amber from Spain: a pluridisciplinary study II" of the Spanish Ministerio de Economía y Competitividad.

## REFERENCES

Alcalá, L., Cobos, A., Delclòs, X., Luque, L., Mampel, L., Royo-Torres, R., after Soriano, C. 2009. Mesozoic terrestrial ecosystems in Teruel. Fundamental, 14, 93-130.

Alonso, J., Arillo, A., Barrón, E., Corral, J.C., Grimalt, J., López, J.F., López, R., Martínez-Delclòs, X., Ortuño, V., Peñalver, E., Trincão, P.R., 2000. A new fossil resin with biological inclusions in Lower Cretaceous deposits from Álava (Northern Spain, Basque-Cantabrian Basin). Journal of Paleontology, 74(1), 158-178.

Arens, N.C., Jahren, A.H., Amundson, R., 2000. Can C3 plants faithfully record the carbon isotopic composition of atmospheric carbon dioxide? Paleobiology, 26(1), 137-164.

Ascaso., C., Wierzchos, J., Corral, J.C., López, R., Alonso, J., 2003. New applications of light and electron microscopic techniques for study of microbiological inclusions in amber. Journal of Palaeontology, 77(6), 1182-1192.

Ascaso, C., Wierzchos, J., Speranza, M., Gutiérrez, J.C., Martín-González, A., De Los Ríos, A., Alonso, J., 2005. Fossil protist and fungi in amber and rock substrates. Micropaleontology, 51(1), 59-72.

Beck, C. W., 1970. Amber in Archaeology. Archaeology, 23, 7-11.

Breton, G., 2007. La bioaccumulation de microorganismes dans l'ambre , analyse comparée d'un ambre cénomanien et d'un ambre sparnacien, et de leurs tapis algaires et bactériens. Comptes Rendus Palevol, 6(1-2), 125-133.

Breton, G., Tostain, F., 2005. Les microorganismes de l'ambre cénomanien d'Écommoy (Sarthe, France). Comptes Rendus Palevol, 4(1-2), 31-46.

Brody, R.H., Edwards, H.G.M., Pollard, A.M., 2001. A study of amber and copal samples using FT-Raman Spectrochimica Acta Part A: Molecular and Biomolecular Spectroscopy, 57(6), 1325-1338.

Cerling, T.E., Harris, J.M., 1999. Carbon isotope fractionation between diet and bioapatite in ungulate mammals and implications for ecological and paleoecological studies. Oecologia, 120, 347-63.

Cervera, A., Pardo, G., Villena, J., 1976, Algunas precisiones litoestratigráficas sobre la Formación "lignitos de Eschucha". Tecniterrae, 3 (14), 25-33.

Chaler, R., Grimalt, J.O., 2005. Fingerprint of Cretaceous higher plant resins by inferred spectroscopy and gas chromatography coupled to mass spectrometry. Phytochemical Analysis, 16(6), 446-450.

Dal Corso, J., Preto, N., Kustatscher, E., Mietto, P., Roghi, G., Jenkyns, H.C., 2011. Carbon-isotope variability of Triassic amber, as compared with wood and leaves (Southern Alps, Italy). Palaeogeography, Palaeoclimatology, Palaeoecology, 302(3-4), 187-193.

Delclòs, X., Arillo, A., Peñalver, E., Barrón, E., Soriano, C., Del Valle, R.L., Bernárdez, E., Corral, C., Ortuño, V.M., 2007. Fossiliferous amber deposits from the Cretaceous (Albian) of Spain. Comptes Rendus Palevol, 6(1-2), 135-149.

Derrick, M.R., Stulik, D., Landry, J.M., 1999. Infrared Spectroscopy in Conservation Science. The Getty Conservation Institute, Los Angeles, 236 pp.

Díez, J.B., Sender, L.M., Villanueva-Amadoz, U., Ferrer, J., Rubio, C., 2005. New data regarding *Weichselia reticulata*: soral cluster and the spore developmental process. Reviews of Palaeobotany and Palynology, 135(1-2), 99-107.

Edwards, H.G.M., Farwell, D.W., 1996. Fourier transform-Raman spectroscopy of amber. Spectrochimica Acta Part A: Molecular and Biomolecular Spectroscopy, 52(9), 1119-1125.

Gomez, B., 2002. A new species of *Mirovia* (Coniferales, Miroviaceae) from the Lower Cretaceous of the Iberian Ranges (Spain). Cretaceous Research, 23(6), 761-773.

Gomez, B., Barale, G., Martín-Closas, C., Thévenard, F., Philippe, M., 1999. Découverte d'une flore à Ginkgoales, Bennettitales et Coniférales dans le Crétacé inférieur de la Formacion Escucha (Chaine Ibérique Orientale, Teruel, Espagne). Neues Jahrbuch für Geologie und Paläontologie, Monatshefte, 11, 661-675.

Gomez, B., Martín-Closas, C., Barale, G., Thévenard, F., 2000. A new species of *Nehvizdya* (Ginkgoales) from the Lower Cretaceous of the Iberian Ranges (Spain). Review of Palaeobotany and Palynology, 111(1-2), 49-70.

Gomez, B., Martín–Closas, C., Méon, H., Thévenard, F., Barale, G., 2001. Plant taphonomy and palaeoecology in the lacustrine Uña delta (Late Barremian, Iberian Ranges, Spain). Palaeogeography, Palaeoclimatology, Palaeoecology, 170, 133-148.

Gomez, B., Martín–Closas, C., Barale, G., Solé de porta, N., Thévenard, F., Guignard, G., 2002. *Frenelopsis* (Coniferales: Cheirolepidiaceae) And Related Male Organ Genera From The Lower Cretaceous Of Spain. Palaeontology, 45(5), 997-1036.

Gomez, B., Coiffard, C., Dépré, É., Daviero-Gomez, V., Néraudeau, D., 2008. Diversity and histology of a plant litter bed from the Cenomanian of Archingeay–Les Nouillers (southwestern France). Comptes Rendus Palevol, 7(2-3), 135-144.

Gradstein, F.M., Ogg, J.G., Schmitz, M., Ogg, G., 2012. The Geologic Time Scale 2012, Elsevier Science Ltd, Oxford, 1176pp.

Guiliano, M., Mille, G., Onoratini, G., Simon, P., 2006. Présence d'ambre dans le Crétacé supérieur (Santonien) de La Mède à Martigues (Sud-Est de la France). Caractérisation IRTF. Comptes Rendus Palevol, 5(7), 851-858.

Guiliano, M., Asia, L., Onoratini, G., Mille, G., 2007. Application of diamond crystal ATR FTIR spectroscopy to the characterization of ambers. Spectrochimica Acta Part A: Molecular and Biomolecular Spectroscopy, 67(5), 1407-1411.

Langenheim, J.H., Beck, C.W., 1965. Infrared spectra as a means of determining botanical sources of amber. Science, 149, 52-55.

McKellar, R.C., Wolfe, A.P., Tappert, R., Muehlenbachs, K., 2008. Correlation of Grassy Lake and Cedar Lake ambers using infrared spectroscopy, stable isotopes, and palaeoentomology. Canadian Journal Of Earth Sciences, 45(9), 1061-1082.

McKellar, R.C., Wolfe, A.P., Muehlenbachs, K., Tappert, R., Engel, M.S., Chen, T., Sánchez-Azofeifa, G. A., 2011. Insect outbreaks produce distinctive carbon isotope signatures in defensive resins and fossiliferous ambers. Proceedings of the Royal Society B, doi:10.1098/rspb.2011.0276.

Menor-Salván, C., Najarro, M., Velasco, F., Rosales, I., Tornos, F., Simoneit, B.R.T., 2010. Terpenoids in extracts of Lower Cretaceous ambers from the Basque-Cantabrian Basin (El Soplao, Cantabria, Spain): Paleochemotaxonomic aspects. Organic Geochemistry, 41(10), 1089-1103.

Murray, A.P., Edwards, D., Hope, J.M., Boreham, C.J., Booth, W.E., Alexander, R.A., Summons, R.E., 1998. Carbon isotope biogeochemistry of plant resins and derived hydrocarbons. Organic Geochemistry, 29(5-7), 1199-1214.

Najarro, M., Peñalver, E., Pérez-De la Fuente, R., Ortega-Blanco, J., Menor-Salván, C., Barrón, E., Soriano, C., Rosales, I., López del Valle, R., Velasco, F., Tornos, F., Daviero-Gomez, V., Gomez, B., Delclòs, X., 2010. Review of the El Soplao Amber Outcrop, Early Cretaceous of Cantabria, Spain. Acta Geologica Sinica, 84(4), 959-976.

Néraudeau, D., Allain, R., Perrichot, V., Videt, B., de Lapparent de Broin, F., Guillocheau, F., Philippe, M., Rage, J.C., Romain Vullo, R., 2003. Découverte d'un dépot paralique à bois fossiles, ambre insectifère et restes d'Iguanodontidae (Dinosauria, Ornithopoda) dans le Cénomanien inférieur de Fouras (Charente-Maritime, Sud-Ouest de la France). Comptes Rendus Palevol, 2(3), 221-230.

Néraudeau, D., Vullo, R., Gomez, B., Perrichot, V., Videt, B., 2005. Stratigraphie et paléontologie (plantes, vertébrés) de la série paralique Albien terminal–Cénomanien basal de Tonnay-Charente (Charente-Maritime, France). Comptes Rendus Palevol, 4, 79-93.

Néraudeau, D., Vullo, R., Gomez, B., Girard, V., Lak, M., Videt, B., Dépré, E., Perrichot, V., 2009. Amber, plant and vertebrate fossils from the Lower Cenomanian paralic facies of Aix Island (Charente-Maritime, SW France). Geodiversitas, 31(1), 13-27.

Néraudeau, D., Manem, S., Delclòs, X., Girard, V., 2011. L'ambre crétacé des Charentes, une alternative à l'ambre balte. In: Marchand, G., Querré, G., (eds.) Roches et Sociétés de la Préhistoire, Rennes, 265-271.

Nissenbaum, A. and Yakir, D., 1995. Stable isotope composition of amber. In: Anderson, K.J., Crelling, J.C., Amber, Resinite, And Fossil Resins, ACS Symposium Series, American Chemical Society, Washington DC, 32-42.

Nissenbaum, A., Yakir, D., Langenheim, J.H., 2005. Bulk carbon, oxygen, and hydrogen stable isotope composition of recent resins from amber-producing *Hymenaea*. Naturwissenschaften, 92(1), 26-29.

Peñalver, E., Delclòs, X., 2010. Spanish Amber. In: Penney, D. (Ed.), Biodiversity of fossils in amber from the major world deposits. Siri Scientific Press, Manchester, 236-270.

Peñalver, E., Delclòs, X., Soriano C., 2007. A new rich amber outcrop with palaeobiological inclusion in the Lower Cretaceous of Spain. Cretaceous Research, 28(5), 791-802.

Peyrot, D., Jolly, D., Barrón, E., 2005a. Apport de données palynologiques à la reconstruction paléoenvironnementale de l'Albo-Cénomanien des Charentes (Sud-Ouest de la France). Comptes Rendus Palevol, 4, 151-165

Peyrot, D., Jolly, D., Barrón, E., 2005b. Nuevas aportaciones a la palinología del Cretácico Inferior de la subcuenca de Oliete (Fm. Escucha, Teruel). Fundamental, 6, 165-168.

Peyrot, D., Rodríguez-López, J.P., Lassaletta, L., Meléndez, N., Barrón, E. 2007a. Contributions to the palaeoenvironmental knowledge of the Escucha Formation in the Lower Cretaceous Oliete sub-basin, Teruel, Spain. Comptes Rendus Palevol, 6(6-7), 469-481.

Peyrot, D., Rodríguez-López, J.P., Barrón, E., Meléndez, N., 2007b. Palynology and biostratigraphy of the Escucha Fomation in the Early Cretaceous Oliete Sub-basin, Teruel, Spain. Revista Española de Micropaleontología, 39(1-2), 135-154.

Querol, X., Salas, R., 1988. El sistema deposicional deltaico del Albiense medio en la Cuenca del Maestrazgo. Cordillera Ibérica Oriental. Extended abstracts: II Congreso Geológico de España, Granada, Sección de Estratigrafía-Sedimentología, 173-176.

Querol, X., Salas, R., Pardo, G., Ardevol, L., 1992. Albian coal-bearing deposits of the Iberian Range in northeastern Spain. Geological Society of America, Special Papers, 267, 193-208.

Ragazzi, E., Roghi, G., Giaretta, A., Gianolla, P., 2003. Classification of amber based on thermal analysis. Thermochimica Acta, 404(1-2), 43-54.

Ragazzi, E., Giaretta, A., Perrichot, V., Néraudeau, D., Schmidt, A.R., Roghi, G., 2009. Thermal analysis of Cretaceous ambers from southern France. Geodiversitas, 31, 163-175.

Schmidt, A.R., Schäfer, U., 2005. *Leptotrichites resinatus* new genus and species, a fossil sheathed bacterium in alpine Cretaceous amber. Journal of Paleontology, 79(1), 175-184.

Schmidt, A.R., Dilcher, D.L., 2007. Aquatic organisms as amber inclusions and examples from modern swamp forest. Proceedings of the National Academy of Sciences, 104(42), 16581-16585.

Schoell, M., Simoneit, B.R., Wang, T., 1994. Organic geochemistry and coal petrology of Tertiary brown coal in Zhoujing mine, Baise Basin, South China – 4: Biomarker sources inferred from stable carbon isotope compositions of individual compounds. Organic Geochemistry, 21(6-7), 713-719.

Sender, L.M., Díez, J.B., Ferrer, J., Pons, D., Rubio, C., 2005. Preliminary data on a new Albian flora from the Valle del Río Martín, Teruel, Spain. Cretaceous Research, 26(6), 898-905.

Stern, B., Lampert Moore C.D., Heron, C., Pollard, A.M., 2008. Bulk stable light isotopic ratios in recent and archaeological resins: towards detecting the transport of resins in antiquity? Archaeometry, 50(2), 351-370.

Villalba-Breva, S., Martín-Closas, C., Marmi, J., Gomez, B., Fernández-Marrón, M.T., 2012. Peat-forming plants in the Maastrichtian coals of the Eastern Pyrenees. Geologica Acta, 10(2), 189-207.

Villanueva-Amadoz, U., Pons, D., Díez, J.B., Ferrer, J., Sender, J.M., 2010. Angiosperm pollen grains of San Just site (Escucha Formation) from the Albian of the Iberian Range (north-eastern Spain). Review of Palaeobotany and Palynology, 162(3), 362-381.

Winkler, W., Kirchner, E.C., Asenbaum, A., Musso, M., 2001. A Raman spectroscopic approach to the maturation process of fossil resins. Journal of Raman Spectrosopy, 32(1), 59–63.

**Manuscript received June 2012;**
**revision accepted April 2013;**
**published Online June 2013.**

# ELECTRONIC APPENDIX

**TABLE I** | Main thermal point (MATHEP) and secondary peaks in DTG profile of amber specimens obtained from main samples SJU6 and SJU8. Aspect and location of fragments: I: Inner, lighter amber portions; P: Peripheral, darker amber portions

| Sample | MATHEP (°C) | Secondary peaks (°C) | Fragment |
|---|---|---|---|
| SJU 6.1 | 409 | 366; 447; 582 | I |
| SJU 6.2 | 409 | 354; 581; 601 | I |
| SJU 6.3 | 417 | 355; 569; 602 | I |
| SJU 6.4 | 420 | 351; 571; 595; 616 | P |
| SJU 8.1A | 450 | 334; 358; 408; 451; 543; 578; 603 | P |
| SJU 8.3A | 429 | 345; 405; 429; 450; 543; 568; 592 | P |
| SJU 8.2G | 421 | 314; 551 | I |
| SJU 8.4G | 430 | 352; 575 | I |

**TABLE II** | Elemental analysis of amber from San Just (in wt%). Data are expressed as mean ± SD of 2-3 replicates. Oxygen and trace elements were determined by difference with the sum of N, C, H and S

| Sample | N | C | H | S | O and trace elements |
|---|---|---|---|---|---|
| SJU6.1 | 0.03±0.01 | 79.29±0.29 | 11.33±0.17 | 0.45±0.04 | 8.91±0.33 |
| SJU6.4 | 0.03±0.01 | 78.20±0.02 | 12.64±0.11 | 0.65±0.05 | 8.50±0.08 |
| SJU8.1A | 0.02±0.01 | 78.69±0.03 | 11.46±0.11 | 0.51±0.01 | 9.32±0.10 |

**TABLE III** | C-isotope composition, colour and preservation of San Just amber. Note the very homogeneous C-isotope signatures of the different analysed portions of SJU 5, 6 and 8 amber specimens. Kind of fragment: I: Inner, lighter amber portions; P: Peripheral, darker amber portions

| Sample | Colour | Fragment | $\delta^{13}C$ ‰ |
|---|---|---|---|
| SJU 5.1 | Orange | I | -22.9 |
| SJU 5.2 | Orange | I | -23.1 |
| SJU 5.3 | Orange | I | -23 |
| SJU 6.1 | Orange | I | -22.9 |
| SJU 6.2 | Orange | I | -22.9 |
| SJU 6.3 | Orange | I | -23 |
| SJU 6.4 | Dark Orange | P | -23.1 |
| SJU 6.5 | Orange | I | -23.3 |
| SJU 6.6 | Orange | I | -23 |
| SJU 7 | Dark Orange | P | -21.1 |
| SJU 8.2G | Orange | I | -22.8 |
| SJU 8.3A | Opaque Yellow-Beige | P | -22.8 |
| SJU 9A | Dark Orange-Red | I | -21.7 |
| SJU 10 | Orange | I | -24 |
| SJU 11 | Orange | I | -21.6 |